# DNA-barcode directed capture and electrochemical metabolic analysis of single mammalian cells on a microelectrode array

**Erik S. Douglas,[a] Sonny C. Hsiao,[b] Hiroaki Onoe,[b] Carolyn R. Bertozzi,[bcd] Matthew B. Francis[bd] and Richard A. Mathies*[abe]**

***Received 3rd December 2008, Accepted 26th March 2009***
***First published as an Advance Article on the web 15th April 2009***
**DOI: 10.1039/b821690h**

A microdevice is developed for DNA-barcode directed capture of single cells on an array of pH-sensitive microelectrodes for metabolic analysis. Cells are modified with membrane-bound single-stranded DNA, and specific single-cell capture is directed by the complementary strand bound in the sensor area of the iridium oxide pH microelectrodes within a microfluidic channel. This bifunctional microelectrode array is demonstrated for the pH monitoring and differentiation of primary T cells and Jurkat T lymphoma cells. Single Jurkat cells exhibited an extracellular acidification rate of 11 milli-pH $min^{-1}$, while primary T cells exhibited only 2 milli-pH $min^{-1}$. This system can be used to capture non-adherent cells specifically and to discriminate between visually similar healthy and cancerous cells in a heterogeneous ensemble based on their altered metabolic properties.

## Introduction

The controlled capture of single cells in microfluidic devices is essential for the development of integrated microdevices for single cell analysis. With size and volume scales comparable to those of individual cells, microfluidic devices provide a powerful tool for control of the cellular microenvironment.[1] Previously we have demonstrated the use of engineered cell surface DNA (cell adhesion barcodes) for cell capture,[2,3] and the use of this capture technique to perform single-cell gene expression analysis in a microfluidic chip.[4] Here we describe the use of DNA barcode cell capture to populate an array of pH-sensitive microelectrodes, enabling the rapid, selective and reversible capture of both adherent and non-adherent single cells on the pH sensor surface. This bifunctional system enables accurate real-time monitoring of single cell metabolism because extracellular acidification is proportional to overall energy usage.[5] We demonstrate the use of this technology to identify cancer cells with high metabolic activity.[6]

Previous work has demonstrated the individual aspects of single cell capture and pH monitoring in microfluidic systems. A variety of methods for arrayed single cell capture have been shown, including physical[7] and energetic traps,[8] and biochemical adhesion.[9,10] While a simple restrictive capture well or microfluidic trap could be used to isolate cells over a sensor, it has been shown that access to fresh media and the ability to clear waste products are important to normal cell function.[11] Furthermore DNA barcodes allow for chemically and physically specific cell capture and enable longer timescale measurements. Highly precise cell placement is also important for monitoring if subcellular-scale electrodes are to be used.[12] The use of extracellular acidification is a valuable tool in the quantitative analysis of cell activity.[13] A key example is the Cytosensor Microphysiometer, which has been widely used to measure acidification from bulk cell populations ($10^4$–$10^6$ cells per 3 μl sample) as a way to quantify metabolism. This system has been used for a number of applications, including the detection of G-protein coupled (chemokine) receptor activation, neurotrophin activity, ligand gated ion channels, and the binding of ligands to tyrosine kinase receptors.[5] It has also been used to identify ligands for orphan receptors.[14] Other devices have also employed pH electrodes to measure cell activity down to the single cell level. Ges *et al.* recently demonstrated a device for on-chip measurement of acidification rates from single cardiac myocytes using physical confinement.[15] In their system, single myocytes were isolated in the sensing volume by physically pinching closed the ends of a PDMS channel. While this system represents an important step in single cell monitoring, the cell isolation technique does not allow for controlled capture on the sensor electrodes, which would be necessary for spatially resolved multi-analyte monitoring from single cells.

The primary goal of the present work is the direct integration of a versatile DNA-based cell capture technique with sensors that are on the same size scale of an individual cell, forming a bifunctional electrode system. To do this, an array of lithographically patterned iridium oxide pH microelectrodes is enclosed within a microfluidic channel. Single stranded DNA is attached to the iridium oxide surface using a silane linker, giving the sensor the ability to capture cells bearing complementary DNA while retaining its detection sensitivity. Here we use this system to measure the extracellular acidification resulting from the metabolism of non-adherent T cells, and we demonstrate that

[a]*UCSF/UC Berkeley Joint Graduate Group in Bioengineering, University of California, Berkeley, California, 94720, USA. E-mail: ramathies@berkeley.edu; Fax: +1 510-642-3599; Tel: +1 510-642-4192*
[b]*Department of Chemistry, University of California, Berkeley, California, 94720, USA*
[c]*Department of Molecular and Cell Biology and Howard Hughes Medical Institute, University of California, Berkeley, California, 94720, USA*
[d]*Materials Sciences Division, Lawrence Berkeley National Laboratory, Berkeley, California, 94720, USA*
[e]*Physical Biosciences Division, Lawrence Berkeley National Laboratory, Berkeley, California, 94720, USA*

 

the pH sensitivity is sufficient to discriminate between healthy primary T cells and cancerous Jurkat T cells that have a higher metabolism. Our results demonstrate the differentiable metabolic activity of individual healthy and transformed cells of the same basic type, which could enable the identification of circulating tumor cells (CTCs) within a heterogeneous sample.[9] The novel combination of DNA-directed cell capture and electrochemical monitoring on a bifunctional electrode offers a new platform for single cell analysis.

## Materials and methods

### Electrode sensor fabrication

Electrodes (40 nm thick Au with a 20 nm Cr adhesion layer) were patterned on 1.1 mm thick borofloat glass wafers using standard photolithographic liftoff, as previously described (Fig. 1).[16] A 7 μm thick layer of Parylene-C was deposited on the wafer using a Specialty Coating Systems Labcoter 2 Parylene deposition system, and measured with an AlphaStep IQ profilometer. A 100 nm layer of aluminum was evaporated on the device, and then lithographically etched using Air Products aluminum etchant with surfactant for 30 s at 60 °C (Fig. 1A, B). The etch mask for the aluminum layer was a photolithographically patterned 1 μm thick film of Shipley 1818 photoresist. The aluminum layer was then used as a mask to etch the underlying Parylene using oxygen plasma (60 sccm $O_2$, 100 W, 60 min).

After removing the Parylene insulation from the sensor area, the sensors were electro-deposited with a layer of iridium oxide following the protocol of Yamanaka.[17] Briefly, the iridium deposition solution was prepared as follows. 37.5 g of $IrCl_4$ was added to 75 mL of de-ionized water and stirred for 90 min. Next, 125 mg of oxalic acid was added, and the solution was stirred for 3 h. Finally, the solution pH was adjusted to 11 using $K_2CO_3$. The solution was initially light yellow, turning light blue, and finally dark blue over the course of several weeks. The deposition solution was stable for at least six months after preparation. Iridium oxide deposition was performed using a CHI 660 potentiostat in voltage cycling mode. 240 cycles of +0.7 V (0.25 s) and −0.5 V (0.25 s) were used, in a three electrode configuration using a saturated calomel reference and a platinum counter electrode.

After deposition, the devices were plasma cleaned for 1 min and modified with trimethoxysilylpropanal by vapor deposition at 60 °C for 60 min. Amine-modified ssDNA (80 μM in phosphate buffered saline) was then deposited onto the devices and bound using reductive amination as previously described[2] (Fig. 1C). Following DNA deposition, the protective aluminum layer was dissolved[18] by treatment with 0.1 M NaOH at room temperature with stirring for 20 min, leaving the capture DNA only on the sensor surface (Fig. 1D).

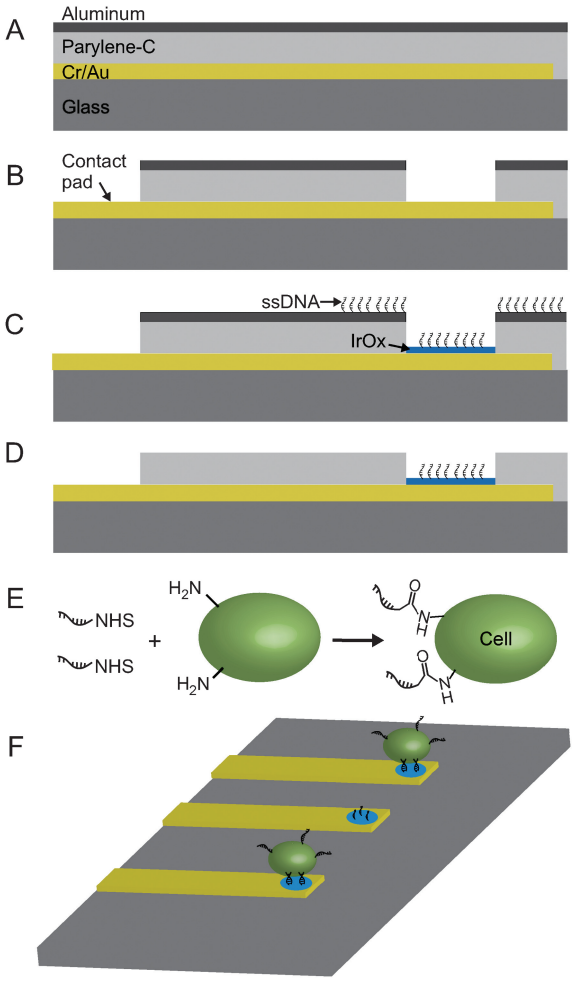


**Fig. 1** Fabrication of the bifunctional microelectrode array for single cell monitoring. (A) Gold electrodes are patterned on a glass wafer using photolithography and liftoff. A 7 μm insulating layer of Parylene-C is then deposited onto the electrodes, and covered with a 100 nm layer of evaporated aluminum. (B) Photoresist is patterned on the aluminum layer, which is then etched and used as an etch mask for the Parylene insulation. (C) The sensor layer of iridium oxide is deposited on the electrode surface and then treated with an aldehyde silane for amine-modified capture DNA attachment. (D) Finally, the aluminum layer is dissolved in strong base, leaving only the capture DNA on the sensor surface. Cells bearing the surface-bound complementary strand are introduced and captured directly and specifically on the sensor. (E) Cells are treated with single stranded DNA (5′-CCCTA-GAGTGAGTCGTATGA-3′) bearing a terminal *N*-hydroxy-succinimidyl (NHS) ester functional group, which binds to primary amines on the cell surface. This DNA barcode labeling functionalizes the cell for DNA-directed capture in the device. (F) Schematic of the microfluidic device. The electrodes are enclosed by a PDMS channel, forming the microfluidic device.

### Microfluidic device preparation

Poly(dimethylsiloxane) (PDMS) channels were prepared using Dow Corning Sylgard 184 with SU-8 or polystyrene molds. Channels were 5 mm wide, 15 mm long, and 600 μm in height. A fluidic inlet compatible with 20 gage Teflon tubing was punched using an 18 gage blunt-tipped needle, and a 5 mm diameter outlet reservoir was punched on the other end. PDMS channels were cleaned with a UV/ozone system for 10 min, and applied to the device. The channels were filled with DI water for 1 h to allow hydration of the iridium oxide layer, then the pH response of the electrodes was calibrated using standard pH 4, 5, 7 and 10 buffers. The channel was maintained at 37 °C using a heated aluminum stage with a MinCO polyimide heater and Cole-Parmer DigiSense PID temperature controller.

### Cell preparation and labeling

Jurkat cells were cultured in RPMI-1640 media with 10% fetal bovine serum (FBS) and 1% penicillin–streptomycin solution. Cultured cells were maintained at 37 °C in 5% $CO_2$, and split 1 : 10 every 2–3 days. Cell acidification experiments were conducted in custom low-buffered media based on Dulbecco's Modified Eagle's Medium, containing 25 mM D-glucose, 5.3 mM KCl, and 110.34 mM NaCl, plus 1% FBS and penicillin/streptomycin. Finally, the media was pH adjusted to 7.45 using 0.1 M NaOH. Primary T cells were the generous gift of Nina Hartman (Jay Groves lab, UC Berkeley Chemistry). Cells were isolated from mice and prepared as previously described.[19]

Cell-surface labeling with ssDNA was achieved using an NHS-DNA conjugate that covalently modifies primary amines on the cell surface (Fig. 1E), as described in Hsiao *et al.*[20] This technique allows for the labeling of primary cells without the three day sugar incubation of our previous work.[3] Briefly, cells were incubated in a 120 μM NHS-DNA solution in PBS at room temperature for 30 min, then washed three times to remove any unbound DNA. Barcode-specific cell capture was tested with spotted DNA microarray slides as previously reported.[2]

### Metabolic monitoring

Cells were suspended at a concentration of $10^6$ $mL^{-1}$, and the suspension was flowed into the microfluidic device. Cell suspensions were flowed into the channel using 1 mL syringes with Teflon tubing. Where Jurkat and primary T cells were monitored simultaneously they were labeled with CellTracker Green and Red dyes, respectively, as previously described[3] and mixed in an equal ratio. Following a 5 min incubation to allow DNA-based cell capture, the unbound cells were rinsed away (5 μl $min^{-1}$ for 3 min) with the low-buffered media. After rinsing, the pH response was monitored electrochemically for 10 min. After this recording, cells were released from the electrodes by heating the device to 55 °C and applying a strong rinse (200 μL $min^{-1}$) with the low-buffered media. Once rinsed and allowed to return to 37 °C, the device could be reloaded with cells. This allowed for multiple measurements to be taken with a single cell preparation.

Voltage measurements were recorded between the iridium oxide electrode and a distant FLEXREF Ag/AgCl reference electrode from World Precision Instruments. An identical iridium oxide electrode outside the cell area was used to compensate for any sensor drift, which was measured to be approximately −0.07 mV $min^{-1}$ (1 micro-pH $min^{-1}$) under experiment conditions. The sensor electrodes were connected to a National Instruments PCI-6031E data acquisition card with a 16 bit analog to digital conversion. The digitized signals were monitored using a custom Labview VI, sampling in multiplex at 3 hz. Voltage signals were processed with a 1% Loess filter using Peak Fit software to reduce noise.

Before metabolic analysis, the electrodes were characterized using standard pH buffers (Fig. 2). These DNA-modified electrodes were found to retain their pH sensitivity, with performance comparable to unmodified iridium oxide sensors. The electrode response was stable and fast, responding to a 1 pH unit change in under 500 ms. The pH response of the electrodes

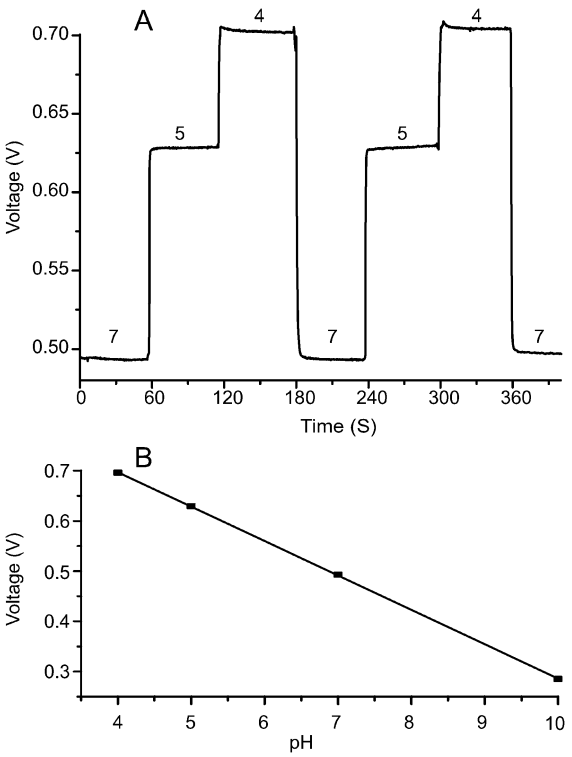


**Fig. 2** Calibration data for the bifunctional microelectrode array. (A) Typical calibration recording for one DNA-modified iridium oxide sensor using standard pH 4, 5 and 7 buffers. Voltage is measured relative to an Ag/AgCl reference electrode. (B) Plot of the voltage *vs.* pH standard measurement with a slope of −68.5 mV/pH unit and $R^2 = 0.99995$.

was typically −68.5 mV per pH unit, with a linear response over the range pH 4 to 10. The typical range for cell acidification measurements is approximately 6.5 to 7.5, so this sensor is well suited for such measurements. The magnitude of the observed response is in line with the −60 to −80 mV $pH^{-1}$ range of other hydrated iridium oxide sensors previously demonstrated.[21–23] The reaction at the electrode that provides the pH sensitivity has been described by Olthuis *et al.*,[24] as shown in eqn (1):

$$2Ir(OH)_2O^- + H_2O \rightleftharpoons Ir_2O(OH)_3O_3^{3-} + 3H^+ + 2e^- \quad (1)$$

The −60 to −80 mV/pH sensitivity range is dependent on the oxidation state of the iridium oxide film as deposited by various electrochemical techniques.

## Results and discussion

The integration of an affinity capture DNA probe with the pH microelectrodes on our bifunctional microelectrode array chip provides a platform for the direct monitoring of extracellular acidification for cells that are normally non-adherent. As seen in Fig. 3, the size-limiting bifunctional microelectrode enables single cell capture directly on the sensor. The bifunctional microelectrode array was tested by measuring the extracellular acidification of Jurkat and primary T cells. First, Jurkat and primary T cells were captured and monitored separately on the array to establish the sensor functionality and the difference in

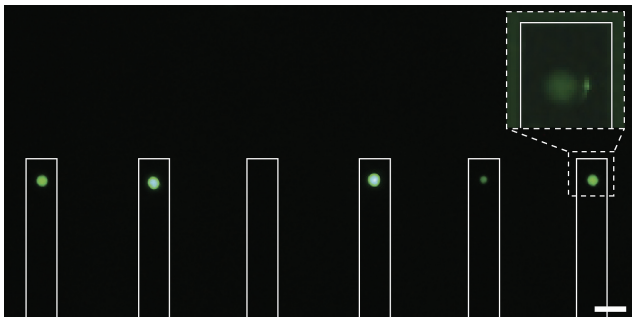

**Fig. 3** Cell capture on the bifunctional microelectrode array. Fluorescent micrograph of individual non-adherent Jurkat cells with a surface-bound DNA barcode bound to the complementary strand on the sensor electrode. Electrode areas are outlined in white. Bar = 40 μm. Inset: magnified view of a single Jurkat cell on an electrode, with additional oblique illumination to reveal the electrode area.

single-cell acidification between the two cell types. Fig. 4A shows single cell acidification data over a 10 min period. Jurkat cells exhibited an extracellular acidification rate of 11.5 ± 3.3 milli-pH $min^{-1}$, while primary T cells exhibited 1.61 ± 1.5 milli-pH $min^{-1}$ (sd, $n = 9$ each). This difference was also confirmed with bulk cell population acidification measurements (~$10^6$ $ml^{-1}$ cells in low-buffered media at 37 °C). Though the primary T cells were murine and the Jurkat cells were of human origin, the salient comparison was mammalian primary *vs.* cancerous T cells.

To demonstrate the ability to distinguish different cells in a mixed population, single cells from a mixture of Jurkat and primary T cells bearing the same cell adhesion barcode were monitored simultaneously on the array. Fig. 4B shows acidification data from mixed cells on the array over 10 min. The difference in measured acidification rates followed the same trend as the separate samples, and allowed for discrimination between the two visually similar cells (Fig. 4B). Jurkat cells had an acidification rate of 10.1 ± 2.3 milli-pH $min^{-1}$, and healthy T cells had 2.41 ± 2.54 milli-pH $min^{-1}$ (sd, $n = 5$ each).

Fig. 4C presents a bar graph of the acidification rates over several trials using known cell populations on the array. For Jurkat cells the mean acidification rate was 11.5 ± 3.2 milii-pH $min^{-1}$, while primary T cells exhibited a rate of 1.62 ± 1.31 milli-pH $min^{-1}$. The difference is clearly significant with a *t*-test value of $P < 0.0002$. While the Jurkat cells were slightly larger than the primary T cells (typically 12 μm *vs.* 10 μm diameter), the size difference is not large enough to account for the difference in acidification.

To demonstrate the ability to measure single cell response to exogenous stimulation, Jurkat cells were treated with rotenone while captured on the bifunctional microelectrode array (Fig. 5). Incubation with rotenone would be expected to interfere with the mitochondrial electron transport chain, causing cells to shift to lactic acid fermentation to complete the glycolytic cycle.[25,26] The resulting excretion of lactic acid should then increase the rate of acidification in the cellular environment.[27] In the experiment, captured cells were first incubated under normal conditions to establish a baseline rate of acidification (~8.8 milli-pH $min^{-1}$) under aerobic metabolism. After 13 min 10 μM rotenone was added to the channel, which resulted in a three-fold increase in the acidification rate (~27.7 milli-pH $min^{-1}$) within 3.5 min. Bulk

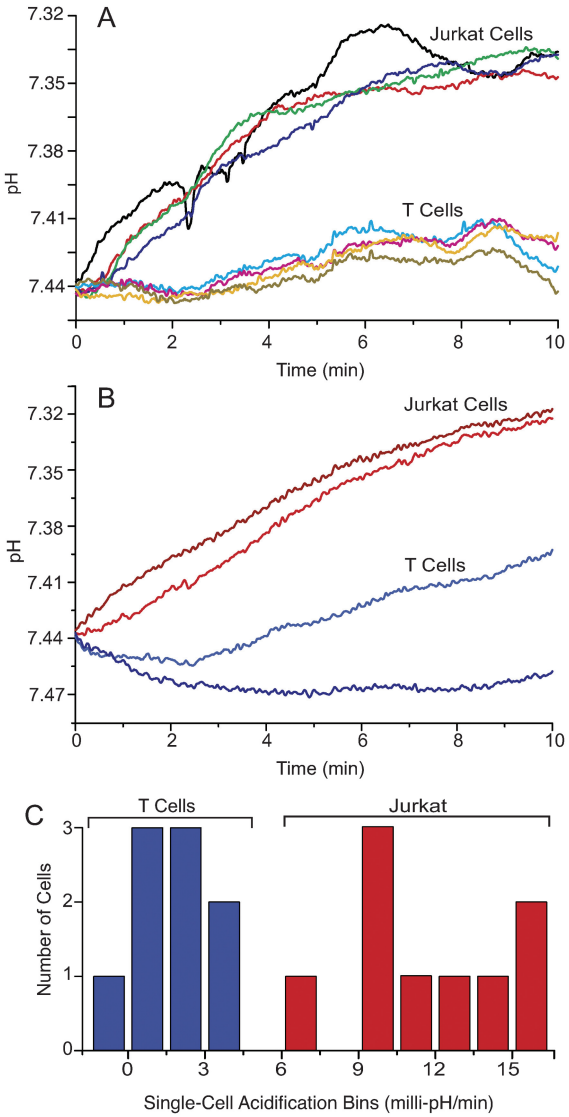


**Fig. 4** Single cell acidification measured with the bifunctional microelectrode array. (A) Representative composite data of single Jurkat and primary T cell acidification measured in known homogenous samples. (B) Single Jurkat and primary T cells captured from a mixture and monitored simultaneously over a 10 min span on the array. (C) Histogram of individual cell acidification in known-type samples over 10 min. Jurkat cells are seen to have a significantly higher ($P < 0.0002$) rate of acidification than primary T cells in low-buffered media.

cell controls, in which Jurkat cells were treated with 1 μM rotenone in low-buffered media (~$10^6$ cells $mL^{-1}$ at 37 °C), consistently demonstrated more than twice the acidification over 60 min compared to identical untreated cells. The observation of this metabolic shift provides an important demonstration of this technique's ability to monitor responses to exogenous agents, such as receptor–ligand binding,[28] at the single cell level.

The bifunctional microelectrode array developed here combines the two important functions of selective cell capture and metabolic monitoring of single cells in an array format. In earlier work, Castellarnau *et al.* used dielectrophoresis to localize high concentration suspensions of bacteria near an ISFET pH sensor and measured the acidification of the cells in the presence

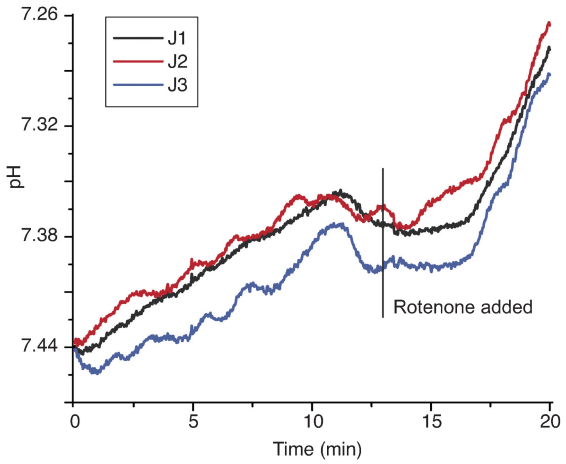


**Fig. 5** Single cell stimulation measured by the bifunctional microelectrode array. Jurkat cells exhibit normal baseline acidification during the first 13 min, then 125 μL of 10 μM rotenone in low-buffered media is added to the channel outlet reservoir where it diffuses into the channel within seconds. Rotenone inhibits the mitochondrial electron transport chain, causing an increased rate of lactic acid excretion, and therefore a higher rate of acidification.

of glucose.[29] While this technique was well suited to measurement of the bulk response, it lacks the ability to resolve the unique activity of single cells. The single cardiac cell pH system of Ges *et al.*[15] provides the ability to monitor large adherent cells, but the volume displacement caused by sealing the channel makes it difficult to direct the cell attachment. DNA-barcode capture provides the advantage of directed capture of both adherent and naturally non-adherent cells, such as T and B cells. This controlled capture provides a platform for spatially-resolved electrical and/or optical probing and measurement of activity on the cell surface. Both of these previous approaches offer the advantage of being able to reuse the device many times, while the Al liftoff technique we employ would make it difficult to selectively reapply capture DNA.

The acidification data show that single non-adherent cells continue to behave normally after treatment with capture DNA and attachment to the electrode. While any capture technique is likely to have some effect on the cell, cell adhesion barcodes bypass the natural cell-surface receptors that are often used for integrin[16] or antibody-based capture,[10] and should thus avoid the activation of those known signaling pathways. For both the Jurkat and primary T cells the extracellular acidification rates measured are comparable to the single cell acidification rates reported by Ges *et al.*[15]

Our single-cell results show that the difference between the metabolic activity of primary non-transformed cells and immortalized cancerous T cells can be detected at the single-cell level. We have demonstrated the ability to electrochemically distinguish between visually similar single cells from the same basic type using this metabolic difference. This methodology could be used to identify individual circulating tumor cells by their distinctive metabolic activity, going beyond simple antibody-based capture.[9] This potential application highlights the value of the NHS-based DNA-labeling technique, which can be readily used with primary cells, and does not require the multi-day incubation of our previous work with unnatural sugars.[3] It could also be used to differentiate between cancerous cells of different metastatic potential.[6] Single-cell monitoring within such a mixture would allow for the detection of differences in drug response based on the cell's state of cancer progression or origin.

The array format with its obvious extension to include more elements allows the direct comparison of the individual activity of many cells under the same conditions with sufficient power to characterize ensemble variation. We are also pursuing the construction of a nanofabricated electrode array that would produce an electrochemical analysis map of a cell surface with high spatial-resolution. Static cell surface profiling has previously been demonstrated using scanning electrochemical microscopy,[30] but a nanoelectrode array could transform this from a serial to a parallel process and provide temporal resolution as well.

Going forward, we are working to add functionality to our single cell analysis by increasing the number of detected analytes from a single cell and the complexity of the analysis system. The previously mentioned Cytosensor Microphysiometer system for bulk cell monitoring was modified to simultaneously measure glucose, lactate and oxygen levels, in addition to the standard pH measurement capabilities.[31] Micro- or nanofabricated analyte-selective sensors could also be added to our system for additional analytical depth, including multi-analyte sensing on a single cell. A combination of calcium-sensitive fluorophores and electrical control has been used to monitor calcium flux in single neurons during patch-clamp recording by Thayer *et al.*[32] Our PDMS/glass multilayer device is readily modified to enable such simultaneous fluorescence and electrical measurements. While fluorescent probes often suffer from photobleaching, our technique could be used to track single-cell metabolic activity over hours or days, revealing any changes as the cell progresses through its life cycle. DNA barcode-based capture also provides the ability to engineer attachment between individual cells in a bio-orthogonal fashion. This could allow for the construction and analysis of discrete multi-type cell systems on an electrode. For example, a single neuron could be linked using DNA to a single muscle cell to allow analysis of the single-cell neuromuscular synaptic formation and operation.[33]

## Conclusions

Our bifunctional microelectrode array provides the ability to selectively capture cells and measure their electrical and metabolic activity. Using DNA-barcode capture, both adherent and naturally non-adherent cells can be studied on the same device. The array format allows us to directly discriminate between cells from a mixture, revealing the variation in single cell properties that make up the ensemble average. This controlled single-cell electrochemical measurement opens the door to the nanoscale cell interface which could enable multiplex, subcellular analysis of cellular activity.

## Acknowledgements

We thank Heather Elsen, Eric Carlson, and Chris Monson for assistance with iridium oxide preparation, and Nicholas Toriello, Zev Gartner and Wilbur Lam for many helpful discussions. E.S.D.

was supported by a National Science Foundation Predoctoral Fellowship. Microfabrication was performed in the UC Berkeley Microlab. This work was supported by the Director, Office of Science, Office of Basic Energy Sciences, of the U.S. Department of Energy under Contract no. DE-AC02-05CH11231.

## References

1 J. El-Ali, P. K. Sorger and K. F. Jensen, *Nature*, 2006, **442**, 403–411.
2 E. S. Douglas, R. A. Chandra, C. R. Bertozzi, R. A. Mathies and M. B. Francis, *Lab Chip*, 2007, **7**, 1442–1448.
3 R. A. Chandra, E. S. Douglas, R. A. Mathies, C. R. Bertozzi and M. B. Francis, *Angew. Chem. Int. Edit.*, 2006, **45**, 896–901.
4 N. M. Toriello, E. S. Douglas, N. Thaitrong, S. C. Hsiao, C. R. Bertozzi, M. B. Francis and R. A. Mathies, *Proc. Nat. Acad. Sci. USA*, 2008, **105**, 20173–20178.
5 F. Hafner, *Biosens. Bioelectron.*, 2000, **15**, 149–158.
6 P. Montcourrier, I. Silver, R. Farnoud, I. Bird and H. Rochefort, *Clin. Exp. Metastasis*, 1997, **15**, 382–392.
7 D. Di Carlo, N. Aghdam and L. P. Lee, *Anal. Chem.*, 2006, **78**, 4925–4930.
8 J. Voldman, *Annu. Rev. Biomed. Eng.*, 2006, **8**, 425–454.
9 S. Nagrath, L. V. Sequist, S. Maheswaran, D. W. Bell, D. Irimia, L. Ulkus, M. R. Smith, E. L. Kwak, S. Digumarthy, A. Muzikansky, P. Ryan, U. J. Balis, R. G. Tompkins, D. A. Haber and M. Toner, *Nature*, 2007, **450**, 1235–1239.
10 D. S. Chen and M. M. Davis, *Curr. Opin. Chem. Biol.*, 2006, **10**, 28–34.
11 A. M. P. Turner, N. Dowell, S. W. P. Turner, L. Kam, M. Isaacson, J. N. Turner, H. G. Craighead and W. Shain, *J. Biomed. Mater. Res.*, 2000, **51**, 430–441.
12 A. F. Dias, G. Dernick, V. Valero, M. G. Yong, C. D. James, H. G. Craighead and M. Lindau, *Nanotechnology*, 2002, **13**, 285–289.
13 H. M. McConnell, J. C. Owicki, J. W. Parce, D. L. Miller, G. T. Baxter, H. G. Wada and S. Pitchford, *Science*, 1992, **257**, 1906–1912.
14 K. Wille, L. A. Paige and A. J. Higgins, *Recept. Channels*, 2003, **9**, 125–131.
15 I. A. Ges, I. A. Dzhura and F. J. Baudenbacher, *Biomed. Microdevices*, 2008, **10**, 347–354.
16 N. M. Toriello, E. S. Douglas and R. A. Mathies, *Anal. Chem.*, 2005, **77**, 6935–6941.
17 K. Yamanaka, *Japan. J. Appl. Phys.*, 1989, **28**, 632–637.
18 B. L. Jackson and J. T. Groves, *Langmuir*, 2007, **23**, 2052–2057.
19 A. L. DeMond, K. D. Mossman, T. Starr, M. L. Dustin and J. T. Groves, *Biophys. J.*, 2008, **94**, 3286–3292.
20 S. C. Hsiao, B. J. Shum, H. Onoe, E. S. Douglas, Z. Gartner, R. A. Mathies, C. R. Bertozzi and M. B. Francis, *Langmuir*, 2009, in press.
21 H. A. Elsen, K. Slowinska, E. Hull and M. Majda, *Anal. Chem.*, 2006, **78**, 6356–6363.
22 S. A. M. Marzouk, R. P. Buck, L. A. Dunlap, T. A. Johnson and W. E. Cascio, *Anal. Biochem.*, 2002, **308**, 52–60.
23 S. A. M. Marzouk, S. Ufer, R. P. Buck, T. A. Johnson, L. A. Dunlap and W. E. Cascio, *Anal. Chem.*, 1998, **70**, 5054–5061.
24 W. Olthuis, M. A. M. Robben, P. Bergveld, M. Bos and W. E. Vanderlinden, *Sensors Actuat. B-Chem.*, 1990, **2**, 247–256.
25 L. J. Mandel, *Curr. Top. Membr. Trans.*, 1986, **27**, 261–291.
26 R. Gebhardt, P. Bellemann and D. Mecke, *Exp. Cell Res.*, 1978, **112**, 431–441.
27 K. L. Tsai, S. M. Wang, C. C. Chen, T. H. Fong and M. L. Wu, *J. Physiol.-London*, 1997, **502**, 161–174.
28 M. F. Renschler, H. G. Wada, K. S. Fok and R. Levy, *Cancer Res.*, 1995, **55**, 5642–5647.
29 M. Castellarnau, N. Zine, J. Bausells, C. Madrid, A. Juarez, J. Samitier and A. Errachid, *Sensors Actuat. B-Chem.*, 2007, **120**, 615–620.
30 T. Kaya, Y. S. Torisawa, D. Oyamatsu, M. Nishizawa and T. Matsue, *Biosens. Bioelectron.*, 2003, **18**, 1379–1383.
31 S. E. Eklund, D. Taylor, E. Kozlov, A. Prokop and D. E. Cliffel, *Anal. Chem.*, 2004, **76**, 519–527.
32 S. A. Thayer, M. Sturek and R. J. Miller, *Pflugers Arch.*, 1988, **412**, 216–223.
33 B. Hoang and A. Chiba, *Dev. Biol.*, 2001, **229**, 55–70.